Journal of Groundwater Science and Engineering
ISSN 2305-7068
Indexed by ESCI CABI CSA
Scopus GeoRef AJ CNKI

Analytical solution for Non-Darcian effect on transient confined-unconfined flow in a confined aquifer

Peng-yu Shi, Jian-jun Liu, Yi-jie Zong, Kai-qing Teng, Yu-ming Huang, Liang Xiao

Citation:
Shi PY, Liu JJ, Zong YJ, *et al*. 2023. Analytical solution for Non-Darcian effect on transient confined-unconfined flow in a confined aquifer. Journal of Groundwater Science and Engineering, 11(4): 365-378.

View online: https://doi.org/10.26599/JGSE.2023.9280029

Journal homepage: http://gwse.iheg.org.cn

Research Paper

Analytical solution for Non-Darcian effect on transient confined-unconfined flow in a confined aquifer

Peng-yu Shi[1,2,3], Jian-jun Liu[1,2,3], Yi-jie Zong[1,2,3], Kai-qing Teng[1,2,3], Yu-ming Huang[1], Liang Xiao[1,2,3*]

[1] *College of Civil Engineering and Architecture*, *Guangxi University*, *Nanning* 530004, *China*.
[2] *Guangxi Key Laboratory of Disaster Prevention and Engineering Safety*, *Guangxi University*, *Nanning* 530004, *China*.
[3] *Key Laboratory of Disaster Prevention and Structural Safety of Ministry of Education*, *Guangxi University*, *Nanning* 530004, *China*.

Abstract: This paper presents a new analytical solution to investigate the mechanism of transient confined-unconfined flow in a confined aquifer induced by pumping with a large rate during mine drainage. The study focuses on understanding the impact of non-Darcian effect on flow towards a fully penetrated pumping well. The nonlinear relationship between specific discharge and the hydraulic gradient is described using Izbash's equation. A novel approximate method is developed to linearize the mathematical model, and the solution is derived using the Boltzmann transform. The proposed solution is validated by comparing it with previous works. The findings indicate that increased non-Darcian index, quasi-hydraulic conductivity, and specific storage have negatively affect the development of the unconfined region and aquifer drawdown, as greater turbulence flow accelerates recharge to the pumping well. Drawdown is found to be sensitive to the non-Darcian index, quasi-hydraulic conductivity, while it is unaffected by specific yield and specific storage. The conclusions provide valuable insights for mine drainage and the application of geological and hydrological conditions.

Keywords: Non-Darcian flow; Izbash equation; Boltzmann transform; Sensitivity analysis

Received: 25 Dec 2022/ Accepted: 30 Apr 2023/ Published online: 15 Jul 2023/ Published: 10 Dec 2023

Introduction

Coal resources account for 94.22% of total primary energy resources in China, leading to significant development in coal mining, particularly in deep coal mining. Deep coal mining operations are typically situated beneath confined aquifer systems and are prone to water inrushes, which have been proven one of the important factors affecting the mining safety (Xiao et al. 2022; Zhao et al. 2021). In order to prevent these water inrushes and ensure mining safety, mine drainage has proven to be a highly effective method for reducing hydraulic pressure in the confined aquifer. However, this drainage process can have detrimental effects on the groundwater resources within the mining area. Consequently, it is crucial to accurately assess the decline in water levels caused by drainage in the confined aquifer to safeguard mine safety and protect groundwater resources in the mining area.

The constant-rate pumping has been widely acknowledged an effective approach for drainage design (Moench et al. 2001; Zong et al. 2022). During the pumping process, if the pumping rate is sufficiently high or the duration of drainage is long enough, the hydraulic head in the confined aquifer can drop below the bottom of the overlying aquitard. This phenomenon leads to the development of a transient unconfined flow near the pumping well. Since 1970s, many analytical and numerical solutions have been proposed to investigate the flow mechanism associated with the transient conversion from confined to unconfined conditions. Moench and Prickett (1972) introduced the MP

*Corresponding author: Liang Xiao, *E-mail address*: xiaoliang850425@sina.com

DOI: 10.26599/JGSE.2023.9280029

Shi PY, Liu JJ, Zong YJ, et al. 2023. Analytical solution for Non-Darcian effect on transient confined-unconfined flow in a confined aquifer. Journal of Groundwater Science and Engineering, 11(4): 365-378.

model and derived an analytical solution with the assumption that the aquifer transmissivity is constant. In the same vein, Elango and Swaminathan (1980) developed a numerical method to study the characteristics of the transient confined-unconfined flow within a confined region. Li et al. (2003) analyzed the mechanism of confined-unconfined flow using both analytical and numerical approaches in an initially dry aquifer. Hu and Chen (2008) presented an analytical solution based on Theis' equation. Wang et al. (2009) extended the MP model and Chen's model to develop a solution for transient conversion flow in a pumping well. Considering the variations in hydraulic properties (such as transmissivity, storativity and diffusivity) between confined and unconfined regions, Xiao et al. (2018) developed an analytical solution. They employed the Boltzmann transform under Darcian conditions. Subsequently, Xiao et al. (2022) utilized a semi-analytical method to investigate the delayed response of drawdown.

Based on a comprehensive literature review, it is noted that previous studies have predominantly assumed Darcian conditions for pumping-induced flow. However, fieldwork and actual experiments have provided evidences of non-Darcian flow occurring in a wide range of porous and fractured media surrounding pumping wells, regardless of the flow rate (e.g. Basak, 1976; Soni et al. 1978; Sen, 1987, 1989, 1990; Bordier and Zimmer, 2000; Wu, 2001, 2002a, 2002b; Moutsopoulos and Tsihrintzis, 2005; Wen et al. 2006, 2011; Houben, 2015; Feng and Wen, 2016; El-Hames, 2020; Jiong et al. 2021; Hao et al. 2021). In term of the non-Darcian flow induced by high pumping rates, two common functions are used to describe the nonlinear specific discharge: The Forchheimer equation and the Izbash's equation. The Forchheimer equation expresses the specific discharge as a second-order polynomial function of hydraulic gradient (e.g. Sen, 1987, 1990; Wu, 2002a; Moutsopoulos and Tsihrintzis, 2005; Mathias and Wen, 2015; Mathias and Moutsopoulos, 2016; Liu et al. 2017), while the Izbash's equation describes the specific discharge as exponentially related to the hydraulic gradient. The Forchheimer equation considers viscous and inertial forces of water flow, and its polynomial form allows flexible representation of flow velocities, regardless of their magnitude (Wen et al. 2008c; Moutsopoulos and Tsihrintzis, 2005). The Izbash's equation is suitable for modelling post-linear non-Darcian flow (Wen et al. 2009; Chen et al. 2003; Qian et al. 2005), and can be more easily linearized in comparison with the Forchheimer equation. Over the past two decades, the validity of these two functions has been verified through their application in various types of aquifer hydraulic tests. These tests include slug test (Wang et al. 2015; Ji and Koh, 2015), and pumping tests in different aquifer systems such as aquifer-aquitard system (Wen et al. 2008a), fractured aquifers (Wen et al. 2006), leaky aquifers (e.g. Wen et al. 2011; Wen and Wang, 2013; Wang et al. 2015), unconfined aquifers (Bordier and Zimmer, 2000; Mathias and Wen, 2015; Moutsopoulos, 2007, 2009), and confined aquifers (e.g. Wen et al. 2008b, 2008c, 2013).

The authors have observed that a high discharge rate during well pumping can cause a temporary transition from confined to an unconfined state in a confined aquifer (e.g. Chen et al. 2006; Wang et al. 2009; Mawlood and Mustafa, 2016; Xiao et al. 2018, 2020, 2023). Additionally, it has also been reported that a large pumping rate can result in non-Darcian flow within the aquifer with a high Reynolds number (R_{ec}>10). Consequently, the drawdown in a confined aquifer induced by a high pumping rate is expected to be influenced by both the non-Darcian flow and transient confined-unconfined conversion. However, to date, there has been a lack of research on groundwater modelling on the transient confined-unconfined flow under non-Darcian conditions.

The paper presents an analytical solution for modelling the transient confined-unconfined flow under non-Darcian conditions. The flow in a confined region is described by a two-dimensional differential equation that represents the seepage system, while the flow in an unconfined region follows the Boussinesq equation with distinct hydraulic parameters. The boundary conditions in the conversion interface are expressed by the flow continuity. To capture the nonlinear relationship between specific discharge and hydraulic gradient, the Izbash's equation is employed for modelling purposes. The analytical solution is obtained by using the Boltzmann transform, which enables the development of a practical approach for assessing the dynamic development of the unconfined region in real-world scenarios. The time-drawdown curves are used to quantify the effect of the non-Darcian index and other hydraulic parameters, and a normalized sensitivity analysis is conducted to evaluate the response of drawdown to the different hydraulic parameters.

1 Model description and solutions

1.1 Conceptual-mathematical model

Fig. 1 illustrates a schematic diagram of pumping test resulting from the transient confined-uncon-

fined flow. The modelling assumptions are as follows: (1) The confined aquifer is isotropic and horizontal infinitely; (2) Both pumping and observation wells fully penetrate the confined aquifer; (3) The pumped rate, Q, remains a constant over time; (4) The effective radius of the pumping well is considered infinitesimal.

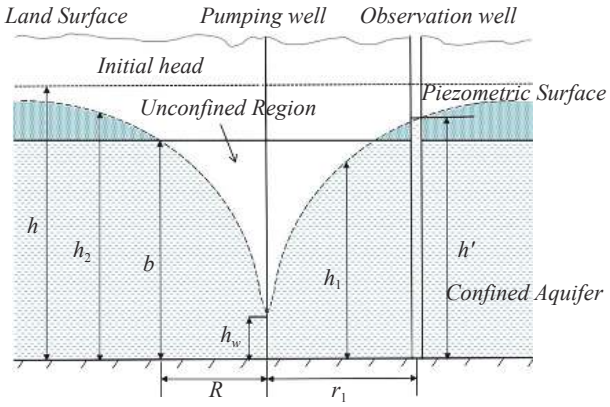

Fig. 1 A schematic diagram of the transient confined-unconfined flow towards a fully penetrating well in a confined aquifer

At the beginning of pumping, the flow from the well is fully confined, and the pumping operation causes the hydraulic head to continuously decrease over time. Once hydraulic head in the pumping well (h_w, L) drops below the bottom of the upper aquiclude (b, L), represented as $0 \leqslant h_w(r,t) \leqslant b$, an unconfined region rapidly develops near the pumping well within the region of $0 < r \leqslant R$, where r denotes the radial distance from the pumping well, L, and R is the radial distance of transient conversion interface from the pumping well, L.

The transient non-Darcian flow in the unconfined region can be described by the Boussinesq equation as follows:

$$\frac{\partial q}{\partial r} + \frac{q}{r} = -\frac{S_y}{h_m}\frac{\partial h_1}{\partial t} \tag{1a}$$

Where: q represents the specific discharge at the radial distance, LT^{-1}; $h_1(r,t)$ is the hydraulic head in the unconfined region, L; h_m is the average hydraulic head of the unconfined region, L; S_y is the specific yield in the unconfined region, and t is the pumping time, T.

The boundary condition representing the fully penetrating well is described as:

$$\lim_{r\to 0} 2\pi r h_1 q = -Q \tag{1b}$$

Where: Q is the pumping rate, L^3T^{-1}.

In the region of $r \geqslant R$, the pumping flow remains under confined condition, and the hydraulic head in the confined region, $h_2(r,t)$, is distributed above the aquifer thickness. This distribution can be expressed as $b \leqslant h_2(r,t) \leqslant h_0$, where h_0 denotes the initial head of the confined aquifer, L. The governing equation can be expressed as (Wen et al. 2008b, 2008c):

$$\frac{\partial q}{\partial r} + \frac{q}{r} = -\frac{S}{b}\frac{\partial h_2}{\partial t} \tag{2a}$$

Where: $S = S_s$ represents the storativity of the confined aquifer and S_s is the specific storage. The boundary condition of the confined region is:

$$h_2(r \to \infty, t) = h_0 \tag{2b}$$

The initial condition is given by:

$$h_1(r,0) = h_2(r,0) = h_0 \tag{3}$$

At the conversion interface between the confined and unconfined regions ($r = R$), the boundary conditions are determined by the flow continuity:

$$\frac{\partial h_1(R,t)}{\partial r} = \frac{\partial h_2(R,t)}{\partial r} \tag{4a}$$

$$h_1(R,t) = h_2(R,t) = b \tag{4b}$$

1.2 Linearization method

Using the Izbash's equation, the nonlinear specific discharge is depicted as:

$$q = \left(-K_r \frac{\partial h}{\partial r}\right)^{\frac{1}{n}} \tag{5}$$

Where: n is defined as the non-Darcian index ranging from 0 to 2, K_r is defined as quasi-hydraulic conductivity, L^nT^{-n}, which are both empirical constants representing the aquifer's water transmission capacity. When $n = 1$, the flow becomes Darcian and K_r becomes hydraulic conductivity (Chen et al. 2003).

By substituting Equation (5) into Equation (2a), we obtain:

$$\frac{n}{r}\left(\frac{\partial h_2}{\partial r}\right) + \left(\frac{\partial^2 h_2}{\partial r^2}\right) = \frac{n}{K_r^{\frac{1}{n}}}\frac{S}{b}\frac{\partial h_2}{\partial t}\left(\frac{\partial h_2}{\partial r}\right)^{\frac{n-1}{n}} \tag{6}$$

Similarly, the governing equation of the unconfined flow can be re-expressed by substituting Equation (5) into Equation (1a) as:

$$\frac{n}{r}\left(\frac{\partial h_1}{\partial r}\right) + \left(\frac{\partial^2 h_1}{\partial r^2}\right) = \frac{n}{K_r^{\frac{1}{n}}}\frac{S_y}{h_m}\frac{\partial h_1}{\partial t}\left(\frac{\partial h_1}{\partial r}\right)^{\frac{n-1}{n}} \tag{7}$$

Assuming that the flow rate in the confined region is equal to Q regardless of the observation well's distance, an approximate can be obtained as (Wen et al. 2008a):

$$\frac{\partial h_2}{\partial r} = \frac{(q)^n}{K_r} \approx \frac{\left(\frac{Q}{2\pi r b}\right)^n}{K_r} \tag{8}$$

Combining Equation (8) with Equation (6) yields:

$$\frac{n}{r}\left(\frac{\partial h_2}{\partial r}\right)+\frac{\partial^2 h_2}{\partial r^2}=\varepsilon_2\frac{\partial h_2}{\partial t}r^{1-n} \tag{9}$$

Where: $\varepsilon_2=\frac{n}{K_r}\frac{S}{b}\left(\frac{Q}{2\pi b}\right)^{n-1}$.

Similar to Equation (8), a linearization approach for Equation (7) is implemented by defining:

$$\frac{\partial h_1}{\partial r}=\frac{(q)^n}{K_r}\approx\frac{\left(\frac{Q}{2\pi r h_m}\right)^n}{K_r} \tag{10}$$

With Equation (10), Equation (7) and (1b) can be re-written as:

$$\frac{n}{r}\left(\frac{\partial h_1}{\partial r}\right)+\frac{\partial^2 h_1}{\partial r^2}=\varepsilon_1\frac{\partial h_1}{\partial t}r^{1-n} \tag{11a}$$

$$\lim_{r\to 0}2\pi r h_1\left(-K_r\frac{\partial h_1}{\partial r}\right)=-Q \tag{11b}$$

Where: $\varepsilon_1=\frac{n}{K_r}\frac{S_y}{h_m}\left(\frac{Q}{2\pi h_m}\right)^{n-1}$.

2 Derivation of analytical solutions

In the section, the solution of the mathematical models for transient confined-unconfined flow is derived using the Boltzmann transform. As shown in Supporting Information, the analytical solution for the transient flow in the unconfined region is given by:

$$h_1(r,t)=b-\left(\frac{Q}{4\pi K_r h_m}\right)\left(\frac{Q}{2\pi r h_m}\right)^{n-1}\left\{W\left[\frac{nS_y r^2}{4tK_r h_m}\left(\frac{Q}{2\pi r h_m}\right)^{n-1}\right]-W\left[\frac{nS_y R^2}{4tK_r h_m}\left(\frac{Q}{2\pi r h_m}\right)^{n-1}\right]\right\} \tag{12}$$

Where: $W(u)$ is the Theis well function.

The hydraulic head in the confined region is expressed as:

$$h_2(r,t)=h_0-\frac{\left(\frac{Q}{2\pi h_m}\right)^n}{2K_r r^{n-1}}\frac{\exp\left[-\frac{nS_y R^2}{4K_r t h_m}\left(\frac{Q}{2\pi R h_m}\right)^{n-1}\right]}{\exp\left[-\frac{nSR^2}{4K_r tb}\left(\frac{Q}{2\pi Rb}\right)^{n-1}\right]}W\left[-\frac{nSr^2}{4K_r tb}\left(\frac{Q}{2\pi Rb}\right)^{n-1}\right] \tag{13}$$

2.1 Drawdown simulation

Using Equations (12) and (13), we have developed an approach to simulate drawdown for transient confined-unconfined flow under non-Darcian conditions in practice. The parameters required for drawdown simulation, including constant pumping rate (Q), initial hydraulic head (h_0), thickness of the confined aquifer (b), and hydraulic parameters (S, S_y, and K_r) of the aquifer, are assumed to be known. The remaining two parameters, the time-depended elevation (h_m) of the piezometric surface in the unconfined region and the radial distance (R) from the transient confined-unconfined interface to the pumping well, can be calculated as follows:

By subjecting the boundary condition Equation (4b) into Equation (13), an expression at the conversion interface can be expressed as:

$$b=h_0-\frac{\left(\frac{Q}{2\pi h_m}\right)^n}{2K_r R^{n-1}}\frac{\exp\left[-\frac{nS_y R^2}{4K_r t h_m}\left(\frac{Q}{2\pi R h_m}\right)^{n-1}\right]}{\exp\left[-\frac{nSR^2}{4K_r tb}\left(\frac{Q}{2\pi Rb}\right)^{n-1}\right]}W\left[-\frac{nSR^2}{4K_r tb}\left(\frac{Q}{2\pi Rb}\right)^{n-1}\right] \tag{14}$$

As shown in Fig. 2, Hu and Chen (2008) considered that the total amount of groundwater drained to the pumping well is equal to the changes of groundwater storage of both the confined and unconfined regions. This can be expressed as:

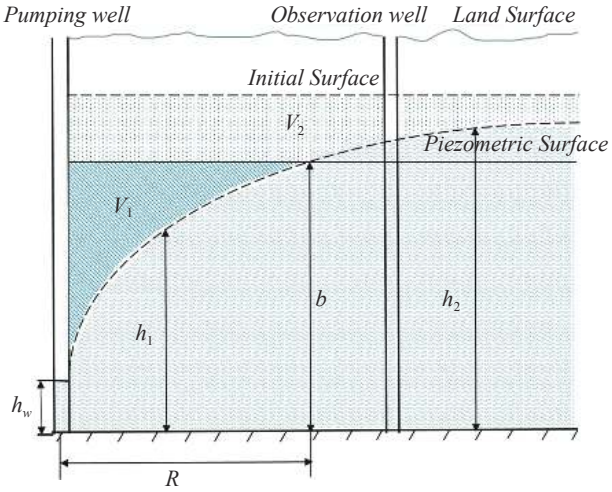

Fig. 2 Change of groundwater storage during the confined-unconfined conversion (after Hu and Chen, 2008)

$$Qt=V_1'+V_2' \tag{15a}$$

Where: V_1' and V_2' are the volume of water pumped from the unconfined region and confined region, respectively. The volume of groundwater pumped from the unconfined region is given by:

$$V_1'=S_y\times V_1,$$

$$V_1 = \int_0^R 2\pi r\,[b - h_1(r,t)]\,dr = \int_0^R 2\pi r\left(\frac{1}{2K_r r^{n-1}}\left(\frac{Q}{2\pi h_m}\right)^n\left\{W\left[\frac{nS_y r^2}{4tK_r h_m}\left(\frac{Q}{2\pi r h_m}\right)^{n-1}\right] - W\left[\frac{nS_y R^2}{4tK_r h_m}\left(\frac{Q}{2\pi r h_m}\right)^{n-1}\right]\right\}\right)dr \tag{15b}$$

Similarly, the volume of groundwater pumped from the confined region is given by:

$$V_2' = S \times V_2,$$

$$V_2 = \pi R^2(h_0 - b) + \int_R^\infty 2\pi r[h_0 - h_2(r,t)]dr = \pi R^2(h_0 - b) + \int_R^\infty 2\pi r\left\{\frac{\left(\frac{Q}{2\pi h_m}\right)^n}{2K_r R^{n-1}}\frac{exp\left[-\frac{nS_y R^2}{4K_r t h_m}\left(\frac{Q}{2\pi R h_m}\right)^{n-1}\right]}{exp\left[-\frac{nSR^2}{4K_r tb}\left(\frac{Q}{2\pi Rb}\right)^{n-1}\right]}W\left[-\frac{nSR^2}{4K_r tb}\left(\frac{Q}{2\pi Rb}\right)^{n-1}\right]\right\}dr \tag{15c}$$

Substituting Equations (15b) and (15c) into Equation (15a) yields:

$$Qt = S_y\int_0^R 2\pi r\left(\frac{1}{2K_r r^{n-1}}\left(\frac{Q}{2\pi h_m}\right)^n\left\{W\left[\frac{nS_y r^2}{4tK_r h_m}\left(\frac{Q}{2\pi r h_m}\right)^{n-1}\right] - W\left[\frac{nS_y R^2}{4tK_r h_m}\left(\frac{Q}{2\pi r h_m}\right)^{n-1}\right]\right\}\right)dr + \left\{\pi R^2(h_0 - b) + \int_R^\infty 2\pi r\left(\frac{\left(\frac{Q}{2\pi h_m}\right)^n}{2K_r R^{n-1}}\frac{exp\left[-\frac{nS_y R^2}{4K_r t h_m}\left(\frac{Q}{2\pi R h_m}\right)^{n-1}\right]}{exp\left[-\frac{nSR^2}{4K_r tb}\left(\frac{Q}{2\pi Rb}\right)^{n-1}\right]}W\left[-\frac{nSR^2}{4K_r tb}\left(\frac{Q}{2\pi Rb}\right)^{n-1}\right]\right)dr\right\} \tag{16}$$

Using Equations (14) and (16), the unknown values of R and h_m can be simulated at each time point of interest.

2.2 Parameter estimations

The pumping test has been widely acknowledged as an effective method for assessing aquifer hydraulic parameters. By analyzing drawdown data obtained from fieldwork, an inversed analytical approach has been developed to determine the dynamic behavior of the unconfined region, as well as the diffusivity and specific yield of unconfined region under confined-unconfined conditions. This approach relies on the assumption that the parameters Q, h_0, b, S, and K_r are known.

As shown in Fig. 2, the unconfined region is radially expanded as pumping continues. The dynamic development of the unconfined region is typically characterized by the radial distance (R) of the conversion interface from the pumping well. Let h_w and $h'(r_1,t)$ represent the water level (measured relative to the bottom of the confined aquifer) in the pumping well and the observation well, respectively. The radial distance between the pumping well and an observation well is denoted as r_1. The transient confined-unconfined conversion flow occurs when the piezometric surface in the pumping well falls below the bottom of the overlying aquitard ($h_w < b$).

During the early pumping stage, the piezometric surface is generally located above the top of the aquifer ($b < h'(r_1,t)$), indicating that the flow towards the observation well is confined. In this case, $h'(r_1,t)$ can be determined by using Equation (13) as:

$$h' = h_0 - \frac{\left(\frac{Q}{2\pi h_m}\right)^n}{2K_r {r_1}^{n-1}}\frac{\exp\left[-\frac{nS_y R^2}{4K_r t h_m}\left(\frac{Q}{2\pi R h_m}\right)^{n-1}\right]}{\exp\left[-\frac{nSR^2}{4K_r tb}\left(\frac{Q}{2\pi Rb}\right)^{n-1}\right]}W\left[-\frac{nS{r_1}^2}{4K_r tb}\left(\frac{Q}{2\pi Rb}\right)^{n-1}\right] \tag{17}$$

Considering the flow continuity and the Equation (4a), the expression at the transient interface can be obtained using Equation (13) as:

$$b = h_0 - \frac{\left(\frac{Q}{2\pi h_m}\right)^n}{2K_r R^{n-1}}\frac{\exp\left[-\frac{nS_y R^2}{4K_r t h_m}\left(\frac{Q}{2\pi R h_m}\right)^{n-1}\right]}{\exp\left[-\frac{nSR^2}{4K_r tb}\left(\frac{Q}{2\pi Rb}\right)^{n-1}\right]}W\left[-\frac{nSR^2}{4K_r tb}\left(\frac{Q}{2\pi Rb}\right)^{n-1}\right] \tag{18}$$

By combining Equations (17) and (18) and taking the ratio, it can be obtained:

$$\frac{h_0 - h'}{h_0 - b} = \frac{R^{n-1}}{{r_1}^{n-1}}\frac{W\left[-\frac{nS{r_1}^2}{4K_r tb}\left(\frac{Q}{2\pi Rb}\right)^{n-1}\right]}{W\left[-\frac{nSR^2}{4K_r tb}\left(\frac{Q}{2\pi Rb}\right)^{n-1}\right]} \tag{19}$$

Based on Equation (19), there are only two unknown parameters: R and t. Therefore, given a specific time point of interest, we can calculate the

R-value in the confined region by finding the root of Equation (19). Once the R-value is determined, the values of specific yield S_y and h_m of the unconfined region can be estimated using Equations (17) and (18).

As the pumping continues, there comes a point where the water level in the observation well falls below the top of the confined aquifer ($h'(r_1,t) < b$) after sufficiently long pumping time. In this scenario, $h'(r_1,t)$ can be calculated using Equation (12), which yields:

$$h' = b - \frac{1}{2K_r {r_1}^{n-1}}\left(\frac{Q}{2\pi h_m}\right)^n \left\{W\left[\frac{nS_y {r_1}^2}{4tK_r h_m}\left(\frac{Q}{2\pi r_1 h_m}\right)^{n-1}\right] - W\left[\frac{nS_y R^2}{4tK_r h_m}\left(\frac{Q}{2\pi r_1 h_m}\right)^{n-1}\right]\right\} \quad (20)$$

By using Equations (16), (18) and (20), the values of R, S_y and h_m can also be assessed for a given pumping time point. In summary, the steps to estimate the pumping test parameters are highlighted as follows: (a) Measure the water level in the observation well; (b) If $b < h'(r_1,t)$ during the early time, employ Equations (17)-(19) to estimate R, S_y and h_m for the confined region; if $h'(r_1,t) < b$, use Equations (16), (18) and (20) to estimate the R, S_y and h_m for the unconfined region.

3 Results and discussion

This section aims to evaluate the validity of the proposed solution by comparing it with the work conducted by Xiao et al. (2018). Additionally, the effects of hydraulic parameters, namely n, K_r and specific storage, on the drawdown and R-value simulation are examined. Considering the assumption that the flow exhibits non-Darcian behavior when $n > 1$, a MATLAB program is employed to numerically simulate the drawdown at specific time of interest using the proposed solution. In general case, the hypothetical values of the parameters are given as within the following ranges: K_r, ranging from 0.0000011574 $m^n s^{-n}$ to 0.00011574 $m^n s^{-n}$ (Wang, 2011); S_y, representing the specific yield of sand and fractured rock aquifers, ranging from 0.05 to 0.5; and S, ranging from 0.000001 to 0.05 (Marsily, 1986).

3.1 Reduction to flow under Darcian condition

Since the proposed analytical solution is intended for non-Darcian flow, it can also be employed to analyze Darcian flow under confined-unconfined conditions by considering a special case when $n = 1$. In this case, the proposed solution can be simplified to describe transient confined-unconfined flow under Darcian condition:

$$h_1(r,t) = b - \frac{Q}{4\pi K_r h_m}\left\{W\left(\frac{nS_y r^2}{4tK_r h_m}\right) - W\left(\frac{nS_y R^2}{4tK_r h_m}\right)\right\} \quad (21)$$

$$h_2(r,t) = h_0 - \frac{Q}{4\pi K_r h_m}\frac{exp\left(-\frac{nS_y R^2}{4K_r t h_m}\right)}{exp\left(-\frac{nSR^2}{4K_r tb}\right)} W\left(-\frac{nSr^2}{4K_r tb}\right) \quad (22)$$

To verify the accuracy of the proposed solution, the results of drawdown simulation using the proposed solution when $n = 1$ are compared to those obtained by Xiao et al. (2018) through a hypothetical case study. The parameter values used in the comparison are as follows: $Q = 0.026$ m^3/s, $K_r = 0.0000695$ m/s, $S_s = 0.000002$ m^{-1}, $S_y = 0.3$, $b = 30$ m, $h_0 = 36$ m and $r_1 = 10$ m. The conversion occurs when the drawdown exceeds 6 m. The simulated time-drawdown curves are presented in Fig. 3. The results indicate that the proposed solution yields nearly identical outcomes to those of Xiao et al. (2018) during the early pumping period. However, slight differences between the two solutions are observed at later stage, likely attributed to the use of different linearization methods. The conversion time, approximately 0.1 day after the start of pumping, supports the acceptability of the proposed solution.

3.2 Effects of *n* constant on drawdown simulation

Fig. 4 illustrates the drawdown curves obtained from a hypothetical study considering different n constants. The parameters used in this study are as follow: $Q = 0.04$ m^3/s, $K_r = 0.0000278$ m/s, $S_s = 0.000002$ m^{-1}, $S_y = 0.3$, $b = 30$ m, $h_0 = 36$ m, $r = 10$ m, $n = 1, 1.1, 1.2$ and 1.3. In this contest, a higher value of n indicates a departure from Darcian flow, where groundwater is more easily transported within the aquifer, leading to a smaller drawdown at any given time of interest. Assuming that hydraulic head represents the hydraulic energy per unit weight of water (Wang et al. 2015), an instantaneous decrease in water level within the well implies a loss of hydraulic energy. It is well-known in fluid mechanics that the turbulent flow ($n > 1$) is the most efficient in dissipating hydraulic energy compared to laminar and Darcian flow (Wang et al. 2015). Consequently, a higher value of n corre-

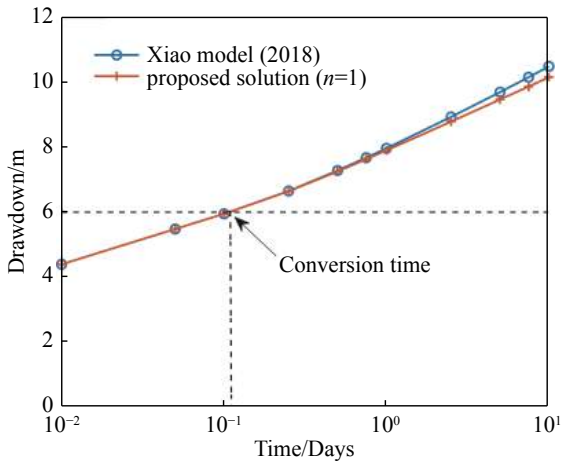

Fig. 3 Comparison of time-Drawdown curves with Xiao's model

Notes: Under the condition of $Q = 0.026\ m^3/s$, K_r =0.0000695 m/s, $S_s = 0.000002\ m^{-1}$, $S_y = 0.3$, $b = 30$ m, $h_0 = 36$ m, $r = 10$ m and $n = 1$ in semi-log scales

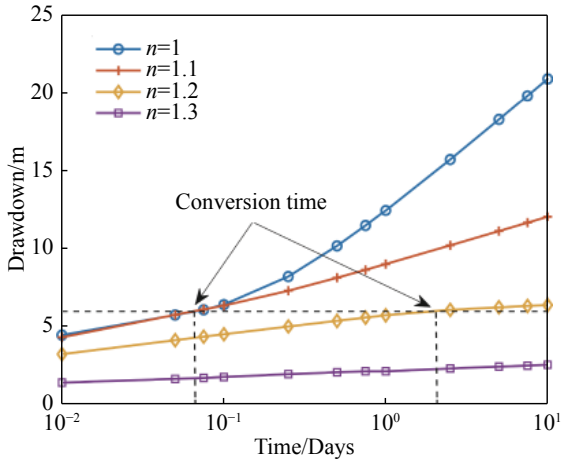

Fig. 4 Time-Drawdown behavior for different index n

Notes: With $Q = 0.04\ m^3/s$, $K_r = 0.0000278$ m/s, $S_s = 0.000002\ m^{-1}$, $b = 30$ m, $h_0 = 36$ m and $r = 10$ m in semi-log scales.

sponds to a higher degree of turbulence flow (Wang et al. 2015), suggesting greater recharge from the area farther away from the pumping well. As a result, a greater n value positively impacts the conversion time while negatively affecting the drawdown. In the case of $n = 1.3$, no confined-unconfined conversion occurs throughout the pumping duration, indicating purely confined flow.

3.3 Effects of S_s on R-Value and drawdown simulation

Fig. 5 depicts the R-time curves of transient confined-unconfined flow under non-Darcian conditions. The curves are generated using the following parameters values: $Q = 0.04\ m^3/s$, K_r = 0.000003475 m/s, $S_y = 0.3$, $b = 30$ m, $h_0 = 36$ m, $r = 10$ m and $n = 1.4$ for three different S_s values of $0.0000016\ m^{-1}$, $0.000002\ m^{-1}$ and $0.0000025\ m^{-1}$. It is important to note that a smaller specific storage results in a larger R value during the early stage. However, as the pumping continues, the R-Time curves for the three different S_s values coincide with each other.

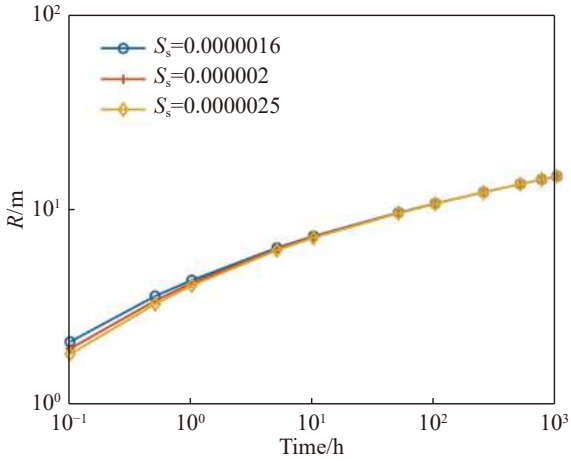

Fig. 5 Time-R value curves for different S_s value

Notes: With $Q = 0.04\ m^3/s$, $K_r = 0.00000348$ m/s, $S_y = 0.3$, $b = 30$ m, $h_0 = 36$ m, $n = 1.4$ and $r = 10$ m in semi-log scales

The time-drawdown curves for the same hypothetical case but with different specific storages are compared in Fig. 6. The differences between three drawdown curves, corresponding to different S_s values, are primarily observed during the early time period. Once the conversion occurs near the observation well, the drawdown curves align with each other, indicating that the S_s value has a negligible influence on drawdown simulation. It can be attributed to the fact that, during the early time, the recharge primarily comes from the elastic storage of the aquifer. A larger S_s value implies a greater release of water from the aquifer, leading to a smaller drawdown at the initial stage. However, the seepage reaches a quasi-stable state towards the end of pumping, the effect of the elastic storage diminishes, exerting no significant impact on the drawdown and R-value of the transient confined-unconfined flow under non-Darcian conditions.

Furthermore, a decreasing slope is observed in the time-drawdown curve from the confined region to the unconfined region. This can be attributed to fact that, at the early pumping stage, the flow predominantly stems from the artesian storage of S_s. As the confined-unconfined conversion takes place, the release of artesian storage gradually decreases, while the discharge of gravity storage represented by S_y is gradually increases. In practice,

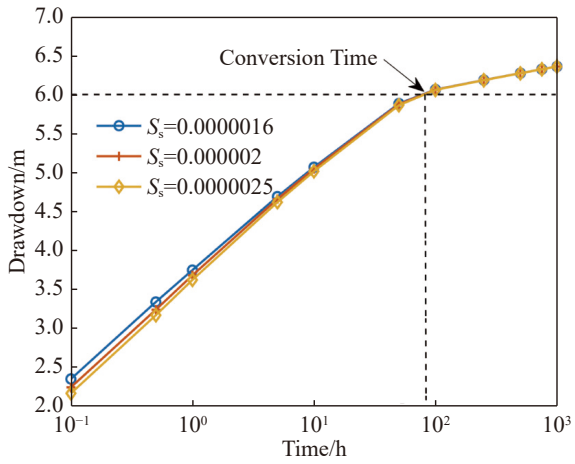

Fig. 6 Time-Drawdown curves for different S_s value

Notes: With $Q = 0.04$ m^3/s, $K_r = 0.00000348$ m/s, $S_y = 0.3$, $b = 30$ m, $h_0 = 36$ m, $n = 1.4$ and $r = 10$ m in semi-log scales

the specific yield is larger than the artesian storage, indicating a greater recharge to the pumping well and a slower decline of water level.

3.4 Effects of K_r constant on R-Value and drawdown simulation

Fig. 7 shows the R-value and drawdown at various time points of interest for the hypothetical scenario of $Q = 0.04$ m^3/s, $S_s = 0.000002$ m^{-1}, $S_y = 0.3$, $b = 30$ m, $h_0 = 36$ m, $r = 10$ m and $n = 1.4$, considering three different K_r values: 0.00000278 m/s, 0.00000348 m/s and 0.00000434 m/s. The findings reveal an inverse relationships between the R and drawdown values as the K_r constant varies. As the pumping continues, the amount of water released from the aquifer gradually decreases, and the recharge predominantly occurs from the regions located further away from the pumping well. With higher K_r values, the flow is more easily transmitted within the aquifer, facilitating faster recharge from outer regions towards the pumped area. Consequently, the development of the unconfined region is constrained, leading to smaller drawdown and delayed conversion from confined flow to unconfined flow.

4 Sensitivity analysis

The objective of the sensitivity analysis is to assess the impact of different parameters on the hydrogeological model and streamline the parameter calibration process. Among the various methods available, local sensitivity analysis has been selected as the calculation approach to evaluate the influence of individual parameters on the analytical solution. In this case, the hydraulic parameters are assumed to be independent of each other. In comparison with Theis' solution, the modeling for transient confined-unconfined flow under non-Darcian conditions involves four key parameters: Quasi-hydraulic conductivity K_r, non-Darcian index n, specific yield S_y, and specific storage S_s. Therefore, conducting a sensitivity analysis becomes necessary.

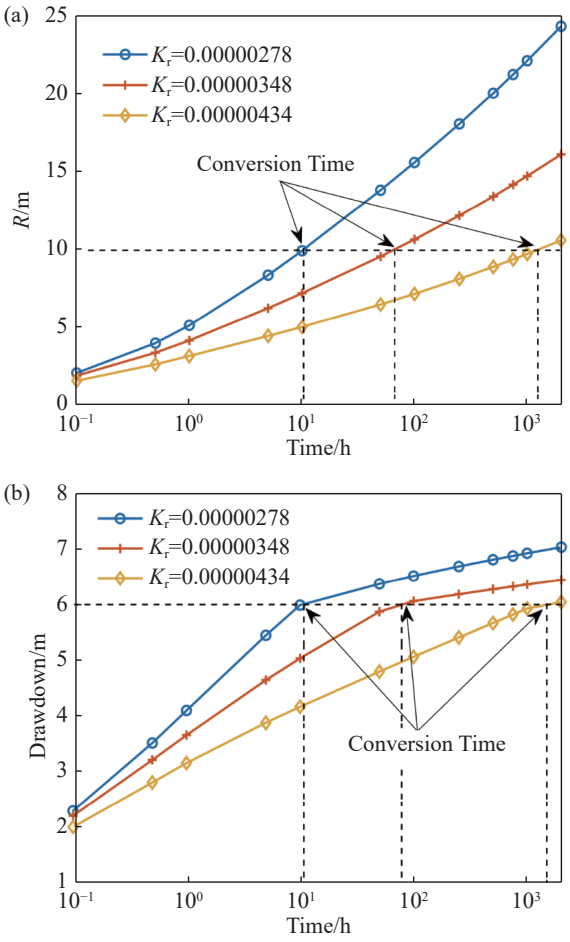

Fig. 7 a) R-time curves and b) time-drawdown curves for different K_r value

Notes: With $Q = 0.04$ m^3/s, $S_y = 0.3$, $S_s = 0.000002$ m^{-1}, $b = 30$ m, $h_0 = 36$ m, $n = 1.4$ and $r = 10$ m in semi-log scales

The sensitivity is defined as a rate of change in one factor with respect to a change in another factor. Based on the work by Huang and Yeh (2007), the normalized sensitivity parameter is defined as:

$$X'_{i,j} = P_j \frac{\partial O_i}{\partial P_j} \tag{23}$$

Where: $X'_{i,j}$ is the normalized sensitivity coefficient of the j-th parameter (P_j) at the i-th time and O_i is the dependent variable of the drawdown. The partial derivation $\frac{\partial O_i}{\partial P_j}$ in Equation (21) is approxi-

mated using a finite difference formula (Huang and Yeh, 2007)

$$X'_{i,j} = P_j \frac{\partial O_i(P_j + \Delta P_j) - \partial O_i(P_j)}{\Delta P_j} \quad (24)$$

Where: ΔP_j is a small increment usually set as $10^{-2} \times P_j$. Fig. 8 illustrates the normalized sensitivity of S_s, S_y, K_r, and n, with $Q = 0.04\ \mathrm{m^3/s}$, $S_s = 0.000002\ \mathrm{m^{-1}}$, $S_y = 0.3$, $b = 30$ m, $h_0 = 36$ m, $r = 10$ m, $n = 1.4$ and $K_r = 0.00000348$ m/s.

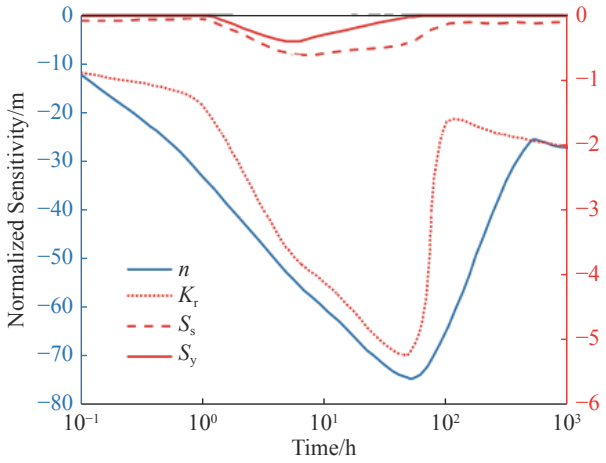

Fig. 8 Sensitivity analysis of aquifer parameters

Notes: With $Q = 0.04\ \mathrm{m^3/s}$, $S_s = 0.000002\ \mathrm{m^{-1}}$, $S_y = 0.3$, b=30 m, $h_0 = 36$ m, $r = 10$ m, $n = 1.4$ and $K_r = 0.000003475$ m/s in semi-log scales

Fig. 8 displays the temporal variation of normalized sensitivity with respect to S_s, S_y, K_r and n values. It is worth noting that the normalized sensitivity of S_s, S_y, K_r and n generally exhibits negative values, indicating a negative relationship. In other word, an increase in S_s, S_y, K_r and n can lead to a decrease in drawdown at the observation well. The normalized sensitivity coefficient curves of K_r and n demonstrate convex shapes, coinciding with the occurrence of conversion from transient confined flow to unconfined flow after approximately 75 hours of pumping. This corresponds to the time when the normalized sensitivity reaches its peak value. This suggests that the normalized sensitivity in the confined region initially decreases with time, but then increases after the confined-unconfined conversion takes place.

5 Conclusions

Greater values of n and K_r result in increased turbulence in flow, which negatively affects the development of the unconfined region and the drawdown of the aquifer. However these values have a positive effect on the time it takes for the conversion from confined to unconfined flow.

A larger specific storage implies a greater release of water from the elastic storage of the aquifer. This initially has a negative impact on the drawdown and the development of the unconfined region during the early stage of pumping. However, as pumping continues, these effects diminish.

The drawdown is particularly sensitive to the power index n and quasi-hydraulic conductivity K_r. The normalized sensitivity of n and K_r in the confined region initially decreases with time, but then increases after the confined-unconfined conversion occurs. On the other hand, the drawdown is not significantly affected by both the specific storage (S_s) and specific yield (S_y).

Nomenclature

Q —constant pumping rate, $\mathrm{L^3T^{-1}}$;
q —specific discharge, $\mathrm{LT^{-1}}$;
K_r —quasi-hydraulic conductivity of the aquifer $\mathrm{L^nT^{-n}}$;
S —storativity coefficient;
S_y —specific yield of the unconfined region;
S_s —specific storage, $\mathrm{L^{-1}}$;
b —the thickness of the confined aquifer, L;
h_0 —initial head, L;
$h_1(r,t)$ —elevation of piezometric surface in unconfined region, L;
$h_2(r,t)$ —elevation of piezometric surface in confined region, L;
$h_m(r,t)$ —effective elevation of piezometric surface within the range from b to zero in the unconfined region, L;
$h'(r,t)$ —elevation of piezometric surface in an observation well, L;
r —radial distance, L;
r_1 —distance of observation well from pumping well, L;
R— radial distance of conversion interface from pumping well, L;
n —power index, an empirical constant in the Izbash's equation;
t — the pumping time, T;
$W(u)$ —theis well function.

Acknowledgements

This study was supported by the national natural science foundation of China (Grant Numbers 41807197, 2017YFC0405900, and 51469002), the natural science foundation of Guangxi (Grant Numbers 2017GXNSFBA198087, 2018GXNSFAA 138042, and GuiKeAB17195073), and Hebei high level talent funding project (B2018003016).

References

Basak P. 1976. Steady non-Darcian seepage through embankments. Journal of the Irrigation and Drainage Division, 102(4): 435−443. DOI：10.1061/JRCEA4.0001256.

Bordier C, Zimmer D. 2000. Drainage equations and non-Darcian modeling in coarse porous media or geosynthetic materials. Journal of Hydrology, 228: 174−187. DOI：10.1016/S0022-1694(00)00151-7.

Chen CX, Hu LT, Wang XS. 2006. Analysis of stead ground water flow toward wells in a confined-unconfined aquifer. Ground Water, 44(4): 609−612. DOI：10.1111/j.1745-6584.2006.00170.x.

Chen CX, Wan JW, Zhan HB. 2003. Theoretical and experimental studies of coupled seepage-pipe flow to a horizontal well. Journal of Hydrology, 281(1-2): 159−171. DOI：10.1016/S0022-1694(03)00207-5.

Elango K, Swaminathan K. 1980. A finite-element model for concurrent confined-unconfined zones in an aquifer. Journal of Hydrology, 46(3-4): 289−299. DOI：10.1016/0022-1694(80)90082-7.

El-Hames AS. 2020. Development of a simple method for determining the influence radius of a pumping well in steady-state condition. Journal of Groundwater Science and Engineering, 8(2): 11. DOI：10.19637/j.cnki.2305-7068.2020.02.001.

Feng Q, Wen Z. 2016. Non-Darcian flow to a partially penetrating well in a confined aquifer with a finite-thickness skin. Hydrogeology Journal, 24(5): 1287−1296. DOI：10.1007/s10040-016-1389-8.

Hao HB, Lv J, Chen YM, et al. 2021. Research advances in non-Darcian flow in low permeability media. Journal of Groundwater Science and Engineering, 9(1): 83−92. DOI：10.19637/j.cnki.2305-7068.2021.01.008.

Houben GJ. 2015. Review: Hydraulics of water wells-flow laws and influence of geometry. Hydrogeology Journal, 23(8): 1633−1657. DOI：10.1007/s10040-015-1312-8.

Hu LT, Chen CX. 2008. Analytical methods for transient flow to a well in a confined-unconfined aquifer. Ground water, 46(4): 642−646. DOI：10.1111/j.1745-6584.2008.00436.x.

Huang YC, Yeh HD. 2007. The use of sensitivity analysis in on-line aquifer parameter estimation. Journal of Hydrology, 335(3-4): 406−418. DOI：10.1016/j.jhydrol.2006.12.007.

Ji SH, Koh YK. 2015. Nonlinear groundwater flow during a slug test in fractured rock. Journal of Hydrology, 520: 30−36. DOI：10.1016/j.jhydrol.2014.11.039.

Li J, Xia XH, Zhan H, et al. 2021. Non-Darcian flow for an artificial recharge well in a confined aquifer with clogging-related permeability reduction. Advances in Water Resources, 147(8): 103820. DOI：10.1016/j.advwatres.2020.103820.

Liu MM, Chen YF, Zhan HB, et al. 2017. A generalized Forchheimer radial flow model for constant-rate tests. Advances in Water Resources, 107(sep.): 317−325. DOI：10.1016/j.advwatres.2017.07.004.

Marsily GD. 1986. Quantitative hydrogeology. Fontainebleau, France: Pairs School of Mines.

Mathias SA, Wen Z. 2015. Numerical simulation of Forchheimer flow to a partially penetrating well with a mixed-type boundary condition. Journal of Hydrology, 524: 53−61. DOI：10.1016/j.jhydrol.2015.02.015.

Mathias SA, Moutsopoulos KN. 2016. Approximate solutions for Forchheimer flow during water injection and water production in an unconfined aquifer. Journal of Hydrology, 538: 13−21. DOI：10.1016/j.jhydrol.2016.03.048.

Mawlood D, Mustafa J. 2016. Comparison between Neuman (1975) and Jacob (1946) application for analysing pumping test data of unconfined aquifer. Journal of Groundwater Science and Engineering, 4(3): 165−173. DOI：10.21271/zjpas.32.2.2.

Moench AF, Prickett TA. 1972. Radial flow in an infinite aquifer undergoing conversion from artesian to water table conditions. Water Resource Research, 8(2): 494−499. DOI：10.1029/WR008i002p00494.

Moench AF, Garabedian SP, LeBlanc DR. 2001. Estimation of hydraulic parameters from an unconfined aquifer test conducted in a glacial outwash deposit, Cape Cod, Massachusetts. US Geology Survey Professional Paper, (1629): 140.

Moutsopoulos KN, Tsihrintzis VA. 2005. Approximate analytical solutions of the Forchheimer equation. Journal of Hydrology, 309(1-4): 93−103. DOI：10.1016/j.jhydrol.2004.11.014.

Moutsopoulos KN. 2007. One-dimensional unsteady inertial flow in phreatic aquifers, induced by a sudden change of the boundary head. Transport Porous Media, 70(1): 97−125. DOI：10.1007/s11242-006-9086-z.

Moutsopoulos KN. 2009. Exact and approximate analytical solutions for unsteady fully developed turbulent flow in porous media and fractures for time dependent boundary conditions. Journal of Hydrology, 369(1-2): 78−89. DOI：10.1016/j.jhydrol.2009.02.025.

Qian JZ, Zhan HB, Zhao WD. 2005. Experimental study of turbulent unconfined groundwater flow in a single fracture. Journal of Hydrology, 311(1-4): 134−142. DOI：10.1016/j.jhydrol.2005.01.013.

Sen Z. 1987. Non-Darcian flow in fractured rocks with a linear flow pattern. Journal of Hydrology, 92(1-2): 43−57. DOI：10.1016/0022-1694(87)90088-6.

Sen Z. 1989. Non-linear flow toward wells. Journal of Hydrology Engineering, 115(2): 193−209. DOI：10.1061/(ASCE)0733-9429(1989)115:2(193).

Sen Z. 1990. Nonliear radical flow in confined aquifers toward large-dsameter wells. Water Resource Research, 26(5): 1103−1109. DOI：10.1016/0148-9062(90)91166-5.

Soni JP, Islam N, Basak P. 1978. An experimental evaluation of non-Darcian flow in porous media. Jounal of Hydrology, 38(3-4): 231−241. DOI：10.1016/0022-1694(78)90070-7.

Wang QR, Zhan HB, Wang YX. 2015. Non-Darcian effect on slug test in a leaky confined aquifer. Journal of Hydrology, 527: 747−753. DOI：10.1016/j.jhydrol.2015.05.038.

Wang XF. 2011. Fundamentals of hydrogeology. Hydrogeology & Engineering Geology, 38(03): 1. (in Chinese)

Wang XS, Wan L, Hu B. 2009. New approximate solutions of horizontal confined–unconfined flow. Journal of Hydrology (Amsterdam), 376(3-4): 417−427. DOI：10.1016/j.jhydrol.2009.07.050.

Wen Z, Huang GH, Zhan HB. 2006. Non-Darcian flow in a single confined vertical fracture toward a well. Journal of Hydrology, 330(3): 698−708. DOI：10.1016/j.jhydrol.2006.05.001.

Wen Z, Huang GH. Zhan HB. 2008a. Non-Darcian flow to a well in an aquifer–aquitard system. Advances in Water Resources, 31(12): 1754−1763. DOI：10.1016/j.advwatres.2008.09.002.

Wen Z, Huang GH, Zhan HB. 2008b. Two-region non-Darcian flow toward a well in a confined aquifer. Advances in Water Resources, 31(5): 818−827. DOI：10.1016/j.advwatres.2008.01.014.

Wen Z, Huang GH, Zhan HB. 2008c. An analytical solution for non-Darcian flow in a confined aquifer using the power law function. Advances in Water Resources, 31(1): 44−55. DOI：10.1016/j.advwatres.2007.06.002.

Wen Z, Huang GH, Zhan HB. 2009. A numerical solution for non-Darcian flow to a well in a confined aquifer using the power law function. Journal of Hydrology, 364(1/2): 99−106. DOI：10.1016/j.jhydrol.2008.10.009.

Wen Z, Huang GH, Zhan HB. 2011. Non-Darcian flow to a well in a leaky aquifer using the Forchheimer equation. Hydrogeology Journal, 19(3): 563−572. DOI：10.1007/s10040-011-0709-2.

Wen Z, Wang QR. 2013. Approximate analytical and numerical solutions for radial non-Darcian flow to a well in a leaky aquifer with wellbore storage and skin effect. International Journal for Numerical & Analytical Methods in Geomechanics, 37(11): 1453−1469. DOI：10.1002/nag.2091.

Wen Z, Liu K, Chen XL. 2013. Approximate analytical solution for non-Darcian flow toward a partially penetrating well in a confined aquifer. Journal of Hydrology, 498: 124−131. DOI：10.1016/j.jhydrol.2013.06.027.

Wu YS. 2001. Non-Darcy displacement of immiscible fluids in porous media. Water Resource Research, 37(12): 2943−2950. DOI：10.1029/2001WR000389.

Wu YS. 2002a. An approximate analytical solution for non-Darcy flow toward a well in frac-

tured media. Water Resource Research, 38(3): 5−1. DOI：10.1029/2001WR000713.

Wu YS. 2002b. Numerical simulation of single-phase and multi-phase non-Darcy flow in porous and fractured reservoirs. Transport Porous Media, 49(2): 209−240. DOI：10.1023/A:1016018020180.

Xiao L, Guo GH, Chen LH, et al. 2022. Theory of transient confined-unconfined flow in a confined aquifer considering delayed responses of water table. Journal of Hydrology, 2022(608): 127644. DOI：10.1016/j.jhydrol.2022.127644.

Xiao L, Liu JJ, Gan FW, et al. 2023. A semi-analytical solution for transient confined–unconfined flow with non-Darcian effect. Journal of Hydrologic Engineering, 28(5): 04023012. DOI：10.1061/JHYEFF.HEENG-5845.

Xiao L, Ye M, Xu YX. 2018. A new solution for confined-unconfined flow toward a fully penetrating well in a confined aquifer. Groundwater, 56(6): 959−968. DOI：10.1111/gwat.12642.

Zhao RJ, Mao DQ, Liu ZB, et al. 2021. An analysis of sequential water releasing tests of the confined aquifers in a coal mine based on hydraulic tomography. Hydrogeology & Engineering Geology, 48(1): 1−9. (in Chinese) DOI：10.16030/j.cnki.issn.1000-3665.202003024.

Zong YJ, Chen LH, Liu JJ, et al. 2022. Analytical solutions for constant-rate test in bounded confined aquifers with non-Darcian effect. Journal of Groundwater Science and Engineering, 10(4): 311−321. DOI：10.19637/j.cnki.2305-7068.2022.04.001.

Supporting Information

The supporting information section presents the detailed derivation process of the analytical solution for transient unconfined and confined flow under non-Darcian conditions.

The proposed approach utilizes a dimensionless method applied to the governing equation (Equation (1)), and the boundary conditions (Equations (2) and (3)).

$$\frac{\partial q}{\partial r}+\frac{q}{r}=-\frac{S_y}{h_m}\frac{\partial h_1}{\partial t} \tag{25}$$

The boundary condition representing the fully penetrating well is described as

$$\lim_{r\to 0} 2\pi r h_m\left(K_r\frac{\partial h_1}{\partial r}\right)^{\frac{1}{n}}=Q \tag{26}$$

$$h_{1(r=R)}=b \tag{27}$$

Using Izbash's equation, the non-linear relationship between the hydraulic gradient and specific discharge is described as

$$q_1=-\left(K_r\frac{\partial h_1}{\partial r}\right)^{\frac{1}{n}} \tag{28}$$

Then Equation (3) is linearized as

$$\frac{\partial h_1}{\partial r}=\frac{(\mathrm{q})^n}{K_r}\approx-\frac{\left(\frac{Q}{2\pi r \mathrm{h_m}}\right)^n}{K_r} \tag{29}$$

Substituting Equations (4) and (5) into Equation (1) gives

$$\frac{n}{r}\left(\frac{\partial h_1}{\partial r}\right)+\frac{\partial^2 h_1}{\partial r^2}=\varepsilon_1\frac{\partial h_1}{\partial t}r^{1-n} \tag{30}$$

Where: $\varepsilon_1=\frac{n_1}{K_r}\frac{S_y}{h_m}\left(\frac{Q}{2\pi h_m}\right)^{n-1}$

Based on the Boltzmann transform, we give an example as

$$\eta=rt^{-\frac{1}{2}} \tag{31}$$

The parameters in Equation (6) can be depicted as

$$\frac{\partial h_1}{\partial r}=t^{-\frac{1}{2}}\frac{\partial v}{\partial \eta} \tag{32}$$

$$\frac{\partial^2 h_1}{\partial r^2}=t^{-1}\frac{\partial^2 v}{\partial \eta^2} \tag{33}$$

$$\frac{\partial h_1}{\partial t}=-\frac{1}{2}rt^{-\frac{3}{2}}\frac{\partial v}{\partial \eta} \tag{34}$$

Substituting Equations (8) to (10) into Equation (5) gives

$$\frac{\partial^2 V}{\partial \eta^2}+\left(\frac{n}{\eta}+\frac{\varepsilon n r^{1-n}}{2}\right)\frac{\partial V}{\partial \eta}=0 \tag{35}$$

The boundary conditions can be described as

$$\lim_{\eta\to 0}\eta^n\frac{\partial V_1}{\partial \eta}=-\frac{\left(\frac{Q}{2\pi \mathrm{h_m}}\right)^n t^{-\frac{n-1}{2}}}{K_r} \tag{36}$$

$$V_1(\eta_R)=b \tag{37}$$

Integrating Equation (12) gives

$$\frac{\partial V_1}{\partial \eta}=D\eta^{-n}\exp\left(-\frac{\varepsilon_1 r^{1-n}}{4}\eta^2\right) \tag{38}$$

Where: D is constant.

With the boundary condition of Equation (12), it gives that

$$D = -\frac{\left(\frac{Q}{2\pi \mathrm{h_m}}\right)^n t^{-\frac{n-1}{2}}}{K_r} \tag{39}$$

Substituting Equation (15) into Equation (14) gives

$$\frac{\partial V_1}{\partial \eta} = \frac{\left(\frac{Q}{2\pi h_m}\right)^n t^{-\frac{n-1}{2}}}{K_r \eta^{n-1}} \frac{1}{\eta} exp\left(-\frac{\varepsilon_1 r^{1-n}}{4}\eta^2\right) \tag{40}$$

Then it can be calculated that

$$V_1(\eta) = \frac{\left(\frac{Q}{2\pi h_m}\right)^n}{K_r r^{n-1}} \int_0^{\eta} \frac{1}{h} \exp\left(-\frac{\varepsilon_1 r^{1-n}}{4} h^2\right) dh + B \tag{41}$$

Where: D is constant.

With the boundary condition of Equation (13), it gives that

$$B = b - \frac{\left(\frac{Q}{2\pi \mathrm{h_m}}\right)^n}{K_r r^{n-1}} \int_0^{\eta_R} \frac{1}{h} \exp\left(-\frac{\varepsilon_1 r^{1-n}}{4} h^2\right) dh \tag{42}$$

Substituting Equation (18) into Equation (17) gives

$$V_1(\eta) = b - \frac{\left(\frac{Q}{2\pi h_m}\right)^n}{K_r r^{n-1}} \int_{\eta}^{\eta_R} \frac{1}{h} \exp\left(-\frac{\varepsilon_1 r^{1-n}}{4} h^2\right) dh \tag{43}$$

Assuming that $\mathrm{u} = \frac{\varepsilon_1 r^{1-n}}{4} h^2$ gives

$$h_1 = b - \frac{\left(\frac{Q}{2\pi \mathrm{h_m}}\right)^n}{2K_r r^{n-1}} \int_{\frac{nS_y r^2}{4K_r t h_m}\left(\frac{Q}{2\pi r h_m}\right)^{n-1}}^{\frac{nS_y R^2}{4K_r t h_m}\left(\frac{Q}{2\pi r h_m}\right)^{n-1}} \frac{1}{u} exp(-u)\, du \tag{44}$$

$$h_1 = b - \left(\frac{Q}{4\pi K_r h_m}\right)\left(\frac{Q}{2\pi r h_m}\right)^{n-1} \left[\int_{\frac{nS_y r^2}{4K_r t \mathrm{h_m}}\left(\frac{Q}{2\pi r \mathrm{h_m}}\right)^{n-1}}^{\infty} \frac{1}{u} exp(-u)\, du - \int_{\frac{nS_y R^2}{4K_r t \mathrm{h_m}}\left(\frac{Q}{2\pi r \mathrm{h_m}}\right)^{n-1}}^{\infty} \frac{1}{u} exp(-u)\, du\right] = b - \left(\frac{Q}{4\pi K_r h_m}\right)\left(\frac{Q}{2\pi r h_m}\right)^{n-1} \left[W\left(\frac{n_1 S_y r^2}{4K_r t h_m}\left(\frac{Q}{2\pi r h_m}\right)^{n-1}\right) - W\left(\frac{nS_y R^2}{4K_r t h_m}\left(\frac{Q}{2\pi r h_m}\right)^{n-1}\right)\right] \tag{45}$$

The proposed dimensionless method is applied to the governing equation, i.e. Equation (22), three boundary conditions, i.e. Equations (23), (24) and (25).

$$\frac{\partial q}{\partial r} + \frac{q}{r} = -\frac{S}{b}\frac{\partial h_2}{\partial t} \tag{46}$$

The boundary condition representing the fully penetrating well can be described as

$$h_2(\mathrm{r} \to \infty) = h_0 \tag{47}$$

$$\frac{\partial h_1(R,t)}{\partial r} = \frac{\partial h_2(R,t)}{\partial r} \tag{48}$$

$$h_1(R,t) = h_2(R,t) \tag{49}$$

Similar to the work above, the governing equation of the confined aquifer can be calculated as

$$\frac{n}{r}\left(\frac{\partial h_2}{\partial r}\right) + \frac{\partial^2 h_2}{\partial r^2} = \varepsilon_2 \frac{\partial h_2}{\partial t} r^{1-n} \tag{50}$$

Where: $\varepsilon_2 = \frac{n_2}{K_r}\frac{S}{b}\left(\frac{Q}{2\pi b}\right)^{n_2-1}$.

Based on the Boltzmann transform above, Equations (23) - (26) can be re-written as

$$V_2(\eta)(\eta \to \infty) = h_0 \tag{51}$$

$$\frac{\partial V_1}{\partial \eta}_{\eta=\eta_R} = \frac{\partial V_2}{\partial \eta}_{\eta=\eta_R} \tag{52}$$

$$V_1(\eta_R) = V_2(\eta_R) \tag{53}$$

$$\frac{\partial^2 V_2}{\partial \eta^2} + \left(\frac{n}{\eta} + \frac{\varepsilon n r^{1-n}}{2}\right)\frac{\partial V_2}{\partial \eta} = 0 \tag{54}$$

Integrating Equation (30) gives

$$\frac{\partial V_2}{\partial \eta} = E\eta^{-n} \exp\left(-\frac{\varepsilon_2 r^{1-n}}{4}\eta^2\right) \tag{55}$$

Where: E is constant.

With the boundary condition of Equation (28), it gives that

$$E = t^{\frac{1-n}{2}} \frac{\left(\frac{Q}{2\pi \mathrm{h_m}}\right)^n}{K_r} \frac{exp\left(-\frac{nS_y R^2}{4K_r t \mathrm{h_m}}\left(\frac{Q}{2\pi R \mathrm{h_m}}\right)^{n-1}\right)}{exp\left(-\frac{\varepsilon_2 R^{1-n}}{4}\eta_R^2\right)} \tag{56}$$

Substituting Equation (32) into Equation (31) gives

$$\frac{\partial V_2}{\partial \eta} = \frac{\left(\frac{Q}{2\pi \mathrm{h_m}}\right)^n}{r^{n-1} K_r} \frac{exp\left(-\frac{nS_y R^2}{4K_r t h_m}\left(\frac{Q}{2\pi R \mathrm{h_m}}\right)^{n-1}\right)}{exp\left(-\frac{\varepsilon_2 R^{1-n}}{4}\eta_R^2\right)} \eta^{-1} \exp\left(-\frac{\varepsilon_2 r^{1-n}}{4}\eta^2\right) \tag{57}$$

$$V_2(\eta) = \frac{\left(\frac{Q}{2\pi h_m}\right)^n}{r^{n-1} K_r} \frac{exp\left(-\frac{nS_y R^2}{4K_r t h_m}\left(\frac{Q}{2\pi R h_m}\right)^{n-1}\right)}{exp\left(-\frac{\varepsilon_2 R^{1-n}}{4}\eta_R^2\right)} \int_0^{\eta} h^{-1} exp\left(-\frac{\varepsilon_2 r^{1-n}}{4}\eta^2\right) dh + \mathrm{C} \tag{58}$$

Where: C is constant.

Using the boundary condition of Equation (27), it yields:

$$C = h_0 - \frac{\left(\frac{Q}{2\pi h_m}\right)^n}{r^{n-1}K_r} \frac{exp\left(-\frac{n_1 S_y R^2}{4K_r t h_m}\left(\frac{Q}{2\pi R h_m}\right)^{n-1}\right)}{exp\left(-\frac{\varepsilon_2 R^{1-n}}{4}\eta_R^2\right)} \int_0^{\infty} h^{-1} exp\left(-\frac{\varepsilon_2 r^{1-n}}{4}h^2\right) dh \quad (59)$$

Substituting Equation (35) into Equation (34) gives

$$V_2(\eta) = h_0 - \frac{\left(\frac{Q}{2\pi h_m}\right)^n}{r^{n-1}K_r} \frac{exp\left(-\frac{n_1 S_y R^2}{4K_r t h_m}\left(\frac{Q}{2\pi R h_m}\right)^{n-1}\right)}{exp\left(-\frac{\varepsilon_2 R^{1-n}}{4}\eta_R^2\right)} \int_{\eta}^{\infty} h^{-1} exp\left(-\frac{\varepsilon_2 r^{1-n}}{4}h^2\right) dh \quad (60)$$